

Article

# Capacity Optimization of Next-Generation UAV Communication Involving Non-Orthogonal Multiple Access <sup>†</sup>

Mubashar Sarfraz <sup>1</sup>, Muhammad Farhan Sohail <sup>1</sup>, Sheraz Alam <sup>1</sup>, Muhammad Javvad ur Rehman <sup>1</sup>, Sajjad Ahmed Ghauri <sup>2</sup>, Khaled Rabie <sup>3,4,\*</sup>, Hasan Abbas <sup>5</sup> and Shuja Ansari <sup>5</sup>

<sup>1</sup> Department of Electrical Engineering, National University of Modern Languages, Islamabad 44000, Pakistan

<sup>2</sup> School of Engineering and Applied Sciences, ISRA University, Islamabad 44000, Pakistan

<sup>3</sup> Department of Engineering, Manchester Metropolitan University, Manchester M15 6BH, UK

<sup>4</sup> Department of Electrical and Electronic Engineering Technology, University of Johannesburg, Doornfontein, P.O. Box 17011, Johannesburg 2028, South Africa

<sup>5</sup> James Watt School of Engineering, University of Glasgow, Glasgow G12 8LT, UK

\* Correspondence: k.rabie@mmu.ac.uk

<sup>†</sup> This work is also supported in parts by Engineering and Physical Sciences Research Council (Grant no. EP/X525716/1).

**Abstract:** Unmanned air vehicle communication (UAV) systems have recently emerged as a quick, low-cost, and adaptable solution to numerous challenges in the next-generation wireless network. In particular, UAV systems have shown to be very useful in wireless communication applications with sudden traffic demands, network recovery, aerial relays, and edge computing. Meanwhile, non-orthogonal multiple access (NOMA) has been able to maximize the number of served users with the highest traffic capacity for future aerial systems in the literature. However, the study of joint optimization of UAV altitude, user pairing, and power allocation for the problem of capacity maximization requires further investigation. Thus, a capacity optimization problem for the NOMA aerial system is evaluated in this paper, considering the combination of convex and heuristic optimization techniques. The proposed algorithm is evaluated by using multiple heuristic techniques and deployment scenarios. The results prove the efficiency of the proposed NOMA scheme in comparison to the benchmark technique of orthogonal multiple access (OMA). Moreover, a comparative analysis of heuristic techniques for capacity optimization is also presented.

**Keywords:** NOMA; UAV communication; user pairing; altitude optimization; heuristic techniques



**Citation:** Sarfraz, M.; Sohail, M.F.; Alam, S.; Javvad ur Rehman, M.; Ghauri, S.A.; Rabie, K.; Abbas, H.; Ansari, S. Capacity Optimization of Next-Generation UAV Communication Involving Non-Orthogonal Multiple Access. *Drones* **2022**, *6*, 234. <https://doi.org/10.3390/drones6090234>

Academic Editor: Vishal Sharma

Received: 9 August 2022

Accepted: 23 August 2022

Published: 2 September 2022

**Publisher's Note:** MDPI stays neutral with regard to jurisdictional claims in published maps and institutional affiliations.



**Copyright:** © 2022 by the authors. Licensee MDPI, Basel, Switzerland. This article is an open access article distributed under the terms and conditions of the Creative Commons Attribution (CC BY) license (<https://creativecommons.org/licenses/by/4.0/>).

## 1. Introduction

Future wireless communication systems and technologies are expected to provide very high data rates [1], consume very low energy [2], and provide massive connectivity [3] and low latency [4]. Unmanned air vehicles (UAVs) have been used in numerous civil as well as military applications, such as monitoring, surveillance, public safety, and transportation management [5]. The main reasons of these applications are the mobility of UAVs and the low manufacturing costs [6]. In the recent past, UAVs have also been investigated for future cellular networks, data collection in the Internet of things (IoT) networks, mobility support in mm-wave communications, and edge computing [7–9]. In particular, the work in [7] studied the UAV data collection for IoT, its recent advances, and also highlighted some future research issues and challenges. On the other hand, the research paper in [8] provided opportunities for mm-wave in UAV communications. Moreover, the authors of [9] investigated UAV in mobile edge computing by using artificial intelligence. Furthermore, the works in [10–12] have presented different resource optimization algorithms for UAV networks. UAVs act as flying ad hoc base stations (BS) to provide required capacity and reliability demands [13,14]. It provides flexible mobility, allowing users to access information at any time and from any location without the need for a fixed infrastructure.

### 1.1. Related Literature

Power domain NOMA has recently attracted increased attention as a key solution to the issues that next-generation wireless networks face [15]. When compared to orthogonal multiple access (OMA) technologies used in 1G to 5G cellular networks, NOMA is shown to have improved spectrum efficiency while sharing the same spectrum resources with multiple devices [16]. NOMA ensures the fairness, quality of services, and capacity of the systems [17]. By using successive decoding technique, multiple users in NOMA can receive information from transmitters [18]. Recently, researches have significantly investigated the traditional NOMA networks. For example, the work in [19] has applied reinforcement learning for NOMA in mobile edge computing. Similarly, the authors in [20] have exploited NOMA in full-duplex communications systems. Another work [21] has used NOMA in cooperative transportation systems, where energy efficiency is maximized through efficient resource allocation. Moreover, the study in [22] has adopted NOMA in intelligent transportation system.

Similarly, the synergy between aerial communication systems and NOMA may provide improved QoS for the existing cellular/terrestrial communication networks [23,24]. This helps to achieve wide coverage, cost-effectiveness, reliability, and on-demand deployment in cellular communications. Meanwhile, in the literature, non-orthogonal multiple access (NOMA) has been proven to optimize the number of serviced customers while maintaining the maximum traffic capacity for future aerial systems. However, additional research into the combined optimization of UAV altitude, user pairing, and power distribution for the problem of capacity maximization is still in the early stages of development.

Recent research has considered NOMA-based UAV cellular communication to increase the capacity of existing cellular networks. For the various communication models, the authors in [25] addressed the fundamental trade-off between UAV altitude and antenna beamwidth for throughput optimization. The appropriate UAV altitude and antenna beamwidth were found to be fundamentally dependent on the communication model used. The deployment of UAV-BS for optimal profitability in terms of data rate is addressed in [26]. The optimization of UAV position and bandwidth, which was influenced by a user's desire to pay for a specific QoS, was designed to enhance overall throughput. In [27], the authors adapted UAV communication and uplink NOMA to build high-capacity IoT uplink transmission systems, in which UAVs served as airborne base stations for collecting data from IoT nodes. The sum capacity of the vehicular network is maximized [28] by optimizing the location of the UAV for visible light communication (VLC). The authors in [29] considered UAV BS as the substitute for malfunctioning ground BS and aimed to maximize the capacity of the network wherein the exact information of the user location and channel model is unknown. In [30], dynamic programming is used to optimize the trajectory of UAVs to achieve better coverage and maximize the per-user throughput.

The authors in [31] introduced the distributed NOMA (D-NOMA) scheme by exploiting the intergroup gap in channel gains of the users to achieve higher data rates compared to conventional NOMA (C-NOMA). An efficient pairing distance NOMA (EPD-NOMA) is presented in [32], where the authors improved the overall throughput by using the calculated non-maximum coupling distance and compared the performance with different variants of NOMA in terms of user pairing techniques. For a multicell MIMO—NOMA downlink scenario, both power allocation (PA), and user pairing are jointly optimized in [33], to improve energy efficiency. In [34], a user-distribution scenario is discussed where more users are at a greater distance from the BS (with lower channel gains). The authors presented a user pairing scheme wherein a nearby user is paired with two faraway users, resulting in better ergodic sum capacity compared to OMA and C-NOMA. An adaptive user-pairing algorithm considering imperfect successive interference cancellation (SIC) scenario is presented in [35]. The proposed algorithm is shown to have better performance in terms of user data rates compared to different NOMA user pairing schemes. Authors in [36], used joint optimization of user pairing and power allocation in an uplink NOMA communication scenario to maximize the sum capacity as well as data rates of paired users.

Research work in [37], presented a novel UP and PA algorithm based on compressive sensing theory that not only exhibits low complexity but also a higher sum rate.

A summary of the related literature is presented in Table 1. As the researchers have mainly addressed the communication issues like energy efficiency, spectral efficiency, optimal coverage, and capacity optimization in NOMA-UAV communication by using the parameters such as user pairing, power allocation, altitude, position, beamwidth, and channel allocation. A combination of altitude, power allocation, and user pairing is seldom used for a capacity optimization problem. Capacity optimization in NOMA-based UAV communication is gaining popularity among researchers due to its various applications requiring handling short-term erratic traffic demand [13].

**Table 1.** Summary of literature review.

Ref.	OF	UP	PA	AL	PO	BW	CA
[13]	EE	✓	✓	✓	-	-	-
[14]	CCO	-	-	-	-	-	✓
[15]	EE	-	✓	-	-	-	-
[18]	SE	-	✓	-	-	-	-
[24]	F-SM	-	-	✓	-	-	-
[25]	TM	-	-	✓	-	✓	-
[26]	TM	-	-	-	✓	-	✓
[27]	CO	-	✓	-	-	-	✓
[28]	CO	-	-	-	✓	-	-
[29]	CO	-	-	-	✓	-	-
[30]	CCO	-	-	-	✓	-	-
[31]	CO	✓	-	-	-	-	-
[32]	SM	✓	-	-	-	-	-
[33]	EE	✓	✓	-	-	-	-
[34]	SM	✓	-	-	-	-	-
[35]	CO	✓	-	-	-	-	-
[36]	CO	✓	✓	-	-	-	-
[37]	SM	✓	✓	-	-	-	-
[38]	EE, CCO	-	✓	✓	-	-	-
<b>OW</b>	SM	✓	✓	✓	-	-	-

EE, energy efficiency; CCO, coverage & capacity optimization; SE, spectral efficiency; F-SM, fairness & sum rate maximization; TO, throughput maximization; PA, power allocation; AL, altitude; UP, user pairing; PO, position; BW, beamwidth; CA, channel allocation; OF, objective function; **OW**, over work.

### 1.2. Motivation and Contribution

The main motivation of our research is to investigate the effect of optimizing power allocation, user pairing, and altitude on the system capacity. The joint altitude and user pairing with different power allocations are formulated as a mixed-integer, non-linear programming (MINLP) problem and it is solved through an optimization algorithm to maximize the network capacity. The major contributions of the proposed scheme are as follows:

1. The altitude optimization problem is formulated as a convex optimization problem and the optimal altitude is evaluated.
2. The sum user capacity is optimized while satisfying the minimum QoS constraints.

3. The comparative analysis of heuristic algorithms is proposed to optimize the user-pairing matrix.

## 2. System Model

The proposed system model is expressed in Figure 1, where there are  $K$  number of users distributed in a circular region of radius  $R_c$  and communicate with UAV. We assume that the channel state information is known in the network [39,40]. The users are placed randomly, and it is assumed that their current position is  $(x_\psi, y_\psi, 0)$  and UAV-BS is assumed at the centre  $(x_0, y_0)$ . As a result, the horizontal distance between user and the vertical projection of UAV-BS placed at  $(x_0, y_0, H)$  is calculated as

$$D_H = \sqrt{(x_\psi - x_0)^2 + (y_\psi - y_0)^2}. \quad (1)$$

Following that, the distance between the user and the UAV-BS, as well as the corresponding angle of elevation, are calculated as

$$X_\psi = \sqrt{D_H^2 + H^2} \quad (2)$$

$$\theta_\psi = \arctan \frac{H}{D_H}. \quad (3)$$

The air-to-ground (A2G) channel for low-altitude platforms (LAPs) is governed by both the line of sight (LoS) and the strong non-line of sight (NLoS) links generated between the user and the UAV, which is in contrast to the LoS dominated A2G channel for high-altitude platforms [41]. Accordingly, the likelihood of establishing an LoS link between the communicating nodes is proportional to the angle of elevation; hence raising the UAV's height enables higher probability of an LoS communication link with the user on the ground. Importantly, the link between the aerial and ground nodes consists of two separate components defined by the level of scattering observed during the transition from aerial node to the user on the ground. In the first phase, the A2G channel experiences the minimum scattering environment near the UAV, and therefore the transmitted signal faces only a free-space path loss. However, the transmitted signal passes through a high scattering environment near the ground in the second phase of the transmission. Thus, the signal has further losses, termed "excessive losses". The high scattering environment near the ground is enabled by the presence of manmade structures such as high-raised buildings and their respective density on the ground. Accordingly, the probability of establishing an LoS A2G link between the communicating nodes improves as the altitude of UAV-BS increases at a fixed horizontal distance from the user. As a result, the likelihood of an LoS link between the user and the UAV-BS is expressed as

$$Pr_{LOS} = \frac{1}{(1 + \mu \exp(-\nu[\theta_\psi - \mu]))}, \quad (4)$$

where  $\mu$  and  $\nu$  are the scaling factors determined by the environment such as urban, suburban, dense urban, rural etc. Therefore, the probability of NLoS is determined by

$$Pr_{NLOS} = 1 - Pr_{LOS}. \quad (5)$$

Moreover, the path loss between the communicating nodes considering the excessive path loss for the cases of LoS and NLoS is computed as

$$\Gamma = \begin{cases} 10\eta \log(X_\psi) + \kappa_{LOS}, \\ 10\eta \log(X_\psi) + \kappa_{NLOS}, \end{cases},$$

where  $\eta$  is the path loss exponent. Because it is not possible to categorize the established link as either LoS and NLoS without prior terrain information, the overall channel condition is defined by the mean path loss evaluated as

$$\bar{\Gamma}(D_H, H) = Pr_{LOS}\Gamma_{LOS} + Pr_{NLOS}\Gamma_{NLOS}. \tag{6}$$

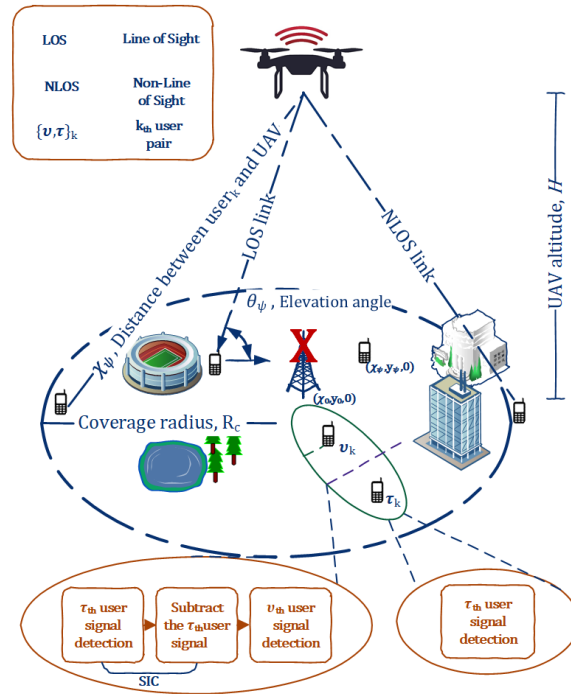


Figure 1. System model.

Transmission Model

In contrast to orthogonal sharing of channel resources employed in OMA, the superimposed transmission of signals from multiple users forms the basis of NOMA. Meanwhile, it is noted that the users selected to form a NOMA pair for simultaneous transmission allows for improved performance when the selected users exhibit distinctive channel conditions. According to (6), the sorted list of channel coefficients of users on the ground with increasing horizontal distance can be presented as  $|h_1|^2 \geq |h_2|^2 \geq \dots \geq |h_N|^2$  [11]. Explicitly, the users experience poor channel conditions as horizontal distance increases. Without loss of generality, let users  $\tau$  and  $v$  be selected to form the  $m$ th pair, where  $1 \leq m \leq M$ . Thus, the superimposed signal for a pair is given as

$$z_\Gamma = \sum_{\Gamma=(\tau,v)_m} \sqrt{P_\Gamma} z_\Gamma, \quad \forall 1 \leq m \leq M, \tag{7}$$

where  $P_\Gamma$  is the transmission power for the  $\tau^{th}$  and  $v^{th}$  users. Next, the received signal at each user is presented as

$$\begin{aligned} y_\tau &= h_\tau (\sqrt{P_\tau} z_\tau + \sqrt{P_v} z_v) + \eta_\tau \\ y_v &= h_v (\sqrt{P_\tau} z_\tau + \sqrt{P_v} z_v) + \eta_v' \end{aligned} \tag{8}$$

where  $\eta_\tau$  represents the noise power and the A2G channel gain  $h_\Gamma$  for each ground user is computed as

$$h_\Psi = \frac{1}{\sqrt{1 + \bar{\Gamma}(D_H, H)}}. \tag{9}$$

An interference-free transmission rate assumes a perfect SIC at the  $\tau$ th user of each pair [42]. On the other hand, the signal for the  $\nu$ th user is decoded without removing the interference from the other constituent of the corresponding pair. Thus, the individual rate of the  $\tau$ th and  $\nu$ th users are represented as

$$Y_\tau = \log_2(1 + P_\tau \Theta_\tau) \quad (10)$$

$$Y_\nu = \log_2 \left( 1 + \frac{P_\nu}{P_\tau + \frac{1}{\Theta_\nu}} \right), \quad (11)$$

where  $\Theta_\tau$  and  $\Theta_\nu$  are given in (12) and (13), and  $P_n$  is the noise power. We have

$$\Theta_\tau = \frac{|h_\tau|^2}{P_n} \quad (12)$$

$$\Theta_\nu = \frac{|h_\nu|^2}{P_n}. \quad (13)$$

Because the proposed scheme assumes a two-user pairing scheme, a user-pairing matrix  $\mathbf{U}$  is defined to ensure that a user can only pair with a single user and a single channel resource block is shared by a maximum of two users. Additionally, the comparison of NOMA performance with that of an equivalent OMA scheme is of paramount importance for a fair analysis. As each user transmits interference-free in its designated time/frequency channel resource, the individual data rate for each OMA user is defined as

$$Y_\Psi^O = \frac{1}{2} \log_2 \left( 1 + \frac{P_{max}}{P_n} |h_\Psi|^2 \right). \quad (14)$$

The scalar factor  $\frac{1}{2}$  in (14) is defined as the multiplexing loss when OMA is assumed for transmission in comparison to the NOMA scheme. Hence, the minimum transmission rate for the proposed problem is constrained to be at least equal to the OMA rate computed at various altitudes of the UAV. Therefore, the main objective is to maximize the total capacity under certain constraints by optimizing the UAV altitude, pairing matrix, and the corresponding power allocation to the NOMA users. The proposed capacity maximization problem is formulated as follows:

$$\begin{aligned} F_k &= \max_{\{U, H_n\}} \sum_{k=1}^K (Y_\tau^k + Y_\nu^k) \\ C_1 &: Y_\Psi^N \geq Y_\Psi^O \quad \forall 1 \leq k \leq K \\ C_2 &: \sum_{k=1}^K u_k = 1, \quad \forall 1 \leq k \leq K \\ C_3 &: \sum_{l=1}^K u_l = 2 \\ C_4 &: p_\tau + p_\nu \leq p^{max} \end{aligned} \quad (15)$$

The constraint  $C_1$  is the individual rate capacity for each NOMA user, which must be equal to or greater than the data rates achievable through OMA for each user in the coverage region. The following constraints  $C_2$  and  $C_3$  is for the user pairing and it shows that the single user must be paired once and there must be maximum of two users in a single resource block, respectively. The maximum transmission power constraint is presented as  $C_4$ , which requires that the sum of powers allocated to  $\tau$ th and  $\nu$ th user must be less than or equal to  $p^{max}$ .

### 3. Proposed Methodology

The objective function of (15) is optimized iteratively through heuristic algorithms, wherein the joint-user pairing matrix  $U$  and UAV height  $H$  is optimized to achieve the above objective. The solution to the formulated problem in (15) requires computation of optimal altitude optimization and the corresponding user pairing scheme to maximize the sum rate capacity of the system. Clearly, the problem of user-pairing optimization is a combinatorial optimization problem which are in general non-convex problems. The exhaustive computation of optimal user pairing for the concerned objective function demands investigation of a large number of user pairs, and it is deemed computationally expensive for any meaningful implementation in a practical aerial NOMA system. Moreover, the proposed altitude optimization to set the best possible combination of channel conditions between the ground users and the UAV to maximize the sum rate of the system translates to a complex optimization without a trivial solution. Therefore, an iterative strategy involving joint optimization of UAV altitude, user pairing and the corresponding power allocation is proposed to solve problem defined in (15). Explicitly, the problem user pairing  $U$  is solved by using meta-heuristic techniques of a genetic algorithm (GA) and particle swarm optimization (PSO). Whereas the problem of altitude  $H_o^N$  optimization, which is a convex optimization given a fixed user-pairing scheme, is solved by using the fmincon optimization tool of Matlab [13]. Meanwhile, the closed-end equations for power allocation for each NOMA user in each pair for sum rate maximization derived from (9) and (10) are given as

$$\log_2(1 + P_\tau \Theta_\tau) \geq Y_\tau^O \quad (16)$$

$$P_\tau \geq \frac{2^{Y_\tau} - 1}{\Theta_\tau} \quad (17)$$

$$1 + \frac{P_v}{P_\tau + \Theta_v} \geq 2^{Y_v^O} \quad (18)$$

$$P_v \geq (2^{Y_v} - 1) \left( P_\tau + \frac{1}{\Theta_v} \right). \quad (19)$$

The proposed algorithm for sum capacity optimization is given in Algorithm 1. The users are divided into two groups, i.e., A & B, according to their distance from BS. Group A users have better channel gains as compared to the group B and are termed as the cell-center users. Similarly, the users in the B group which are farther from the UAV are considered as the cell-edge users. In order to reduce the search space, the user pairing is not allowed between the users of the same group in the proposed scheme. This assumption is also validated by the fact that NOMA performance is better when users with distinctive channel conditions are grouped together [2]. Thus, the users farther from each other are the best candidates for transmitting together as a pair. The user pairing is done when each user is randomly paired with the user of an opposite group. Afterward, the optimal height is obtained through a local search algorithm. Finally, the sum capacity is evaluated for each candidate solution, sorted in descending order, and it is linked with each candidate solution.

The proposed scheme initiates by randomly assigning users from both groups to form the NOMA user pairs. Subsequently, the fmincon tool is invoked to compute optimal altitude given a fixed user pairing. Next, the steps associated with GA/PSO such as cross-over, mutation, and position updates are employed to optimize the user pairing. The objective function of (15) is updated at each step and the optimal solution is evaluated iteratively while satisfying all the constraints. The proposed algorithm runs for the defined number of cycles to output user pairing, altitude, and corresponding power allocation sum rate maximization of the aerial NOMA system.

**Algorithm 1:** Heuristic based joint user-pairing and altitude optimization (HUAO).

---

```

1 Initialize  $\mathbf{U}, H^N, K, \text{SNR}, \eta, GA$  and  $PSO$  parameters
2 get  $Y_{\Psi}^O$ 
3 while  $Y_{\Psi}^N < Y_{\Psi}^O$  do
4   for  $i=1:\frac{K}{2}$  do
5     if  $u_i \neq 1 \parallel u_i \neq 2$  then
6       find pairing  $u_{i,l}$  b/w group  $A$  &  $B$ 
7     end
8   end
9   while  $H^N \neq H_0^N$  do
10    find altitude  $H^N$ 
11    if  $H^{min} \leq H^N \leq H^{max}$  then
12      if  $H^N == H_0^N$  then
13        break;
14      end
15    end
16  end
17 end
18 return  $Y_{\tau}^N, Y_{\nu}^N, H_0^N$ 

```

---

**4. Simulation Results and Discussion**

The detailed analysis of the impact of different user-pairing schemes and SNRs at different altitudes (80m and 120m) on sum rate optimization is presented. The maximum transmission power for a single pair of users is considered 1 watt throughout the simulations. The simulation has been carried out in three different environments: suburban, urban, and dense urban. The objective is to maximize the sum rate through (15) by satisfying the subject constraints, and the comparison of GA- and PSO-based optimization is carried out in this section. Simulation parameters are described in Table 2.

**Table 2.** Simulation parameters.

Parameters	Values
$K$ (users)	20
$N$ (candidate solutions)	20
Crossover	Single point
Selection	Roulette wheel selection
Mutation rate	1 %
$\omega$ (PSO: inertia)	0.7
$C_1, C_2$ (PSO: constants)	Random
$P_{tx}$	1W
$\eta_0$ (Free Space pathloss exponent)	2
<b>Environment</b>	<b>suburban</b> <b>urban</b> <b>dense urban</b>
$\mu$	4.886      9.6177      12.087
$\nu$	0.429      0.1581      0.1139
$\Omega_{LOS}$	0.1      1      1.6
$\Omega_{NLOS}$	21      20      23

Figures 2 and 3 show the comparative analysis of GA- and PSO-based user pairing for all the environments. Altitudes of NOMA-UAV is fixed at 80 m and 120m m for the simulations, and the results of the proposed HUAO algorithm are compared with OMA. Sum rates are optimized through GA- and PSO-based schemes over various iterations. The GA- and PSO-based user pairing in NOMA gives better performance as compared to the OMA. The convergence of PSO is fast as compared to the GA.

Figure 2 shows the performance improvement of the proposed PSO compared to OMA and GA, where 54.05% and 21.61% for suburban, 43.6% and 24.21% for urban, 39.45% and 12.32% improvement for dense urban is achieved. In Figure 3, PSO gives an improvement of 58.3% and 16.7% for suburban, 46.38% and 3.8% for urban, 42.73% and 16.7% for dense urban as compared to OMA and GA, respectively. The overall results show the superiority of the proposed PSO-based user pairing. Therefore, PSO-based pairing is used for the next sections.

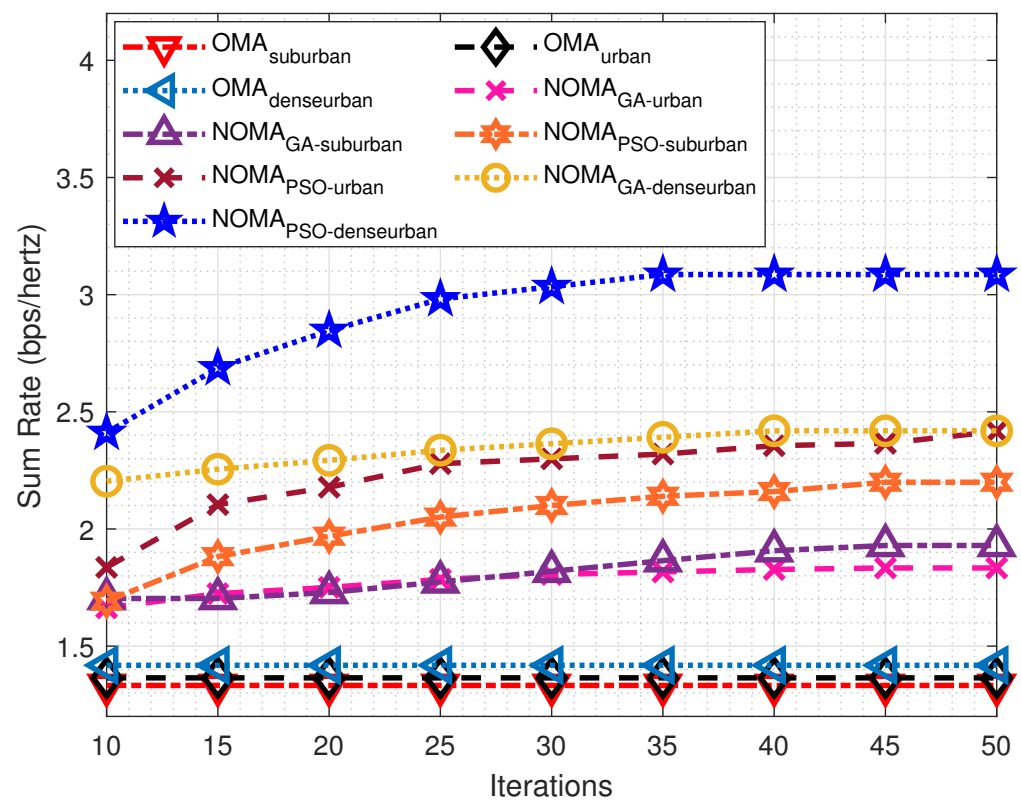


Figure 2. GA- and PSO-based comparative analysis of sum rates: OMA altitude at 80 m.

#### 4.1. Analysis of Pairing Schemes

In this section, three pairing schemes, i.e., adjacent pairing, random pairing and HUAO-based pairing are analyzed with reference to the OMA altitude of 80 m at 20 dB SNR. In adjacent pairing, closed users are paired (with minimum distance), users are paired randomly in random pairing, and HUAO-based pairing is a proposed pairing scheme (as discussed in the proposed methodology section).

Figure 4 presents a comparison of different pairing schemes for the suburban setting. Adjacent pairing gives the performance improvement of 6.8%, and random pairing gives 7.87%. HUAO-based pairing outperforms the other pairing schemes and gives an improvement of 24.75%. Figure 5 shows the analysis of pairing schemes for the urban environment. The performance improvement of adjacent pairing is 6.16%, the random pairing is 8.7%, and HUAO is 25.06%. Figure 6 gives the comparative analysis for the dense urban environment, where adjacent pairing achieves 10.33%, random pairing gives 12.32%, and HUAO gives the performance improvement of 31.97%.

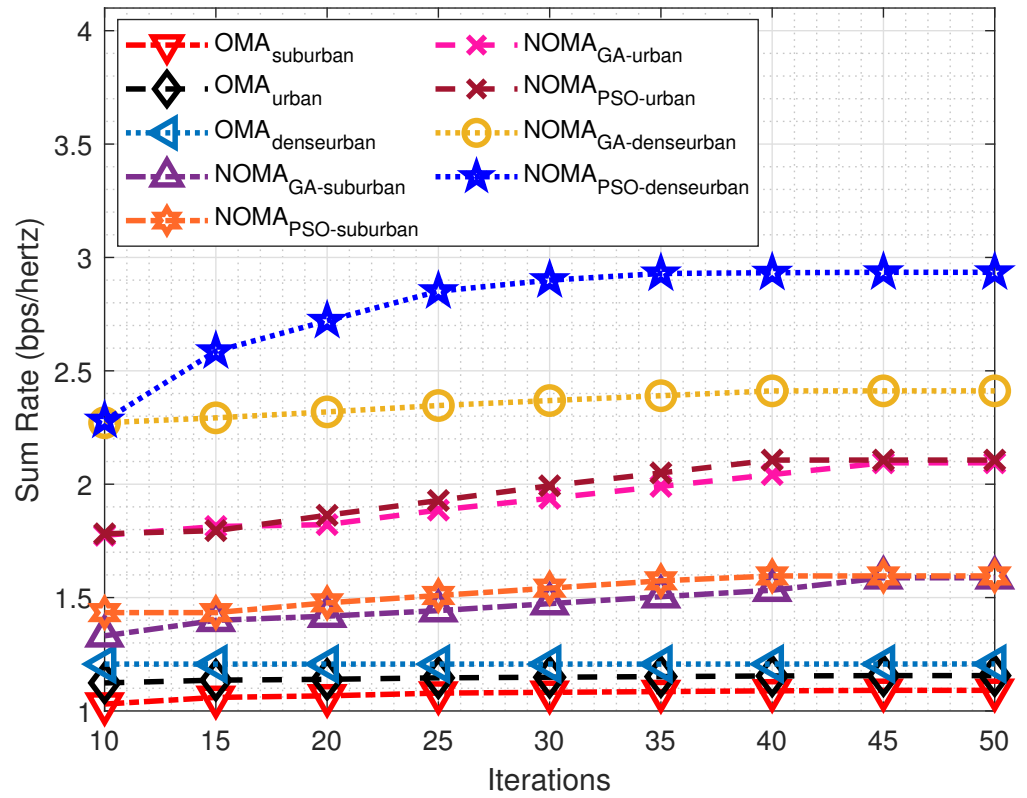


Figure 3. GA- and PSO-based comparative analysis of sum rates: OMA altitude at 120 m.

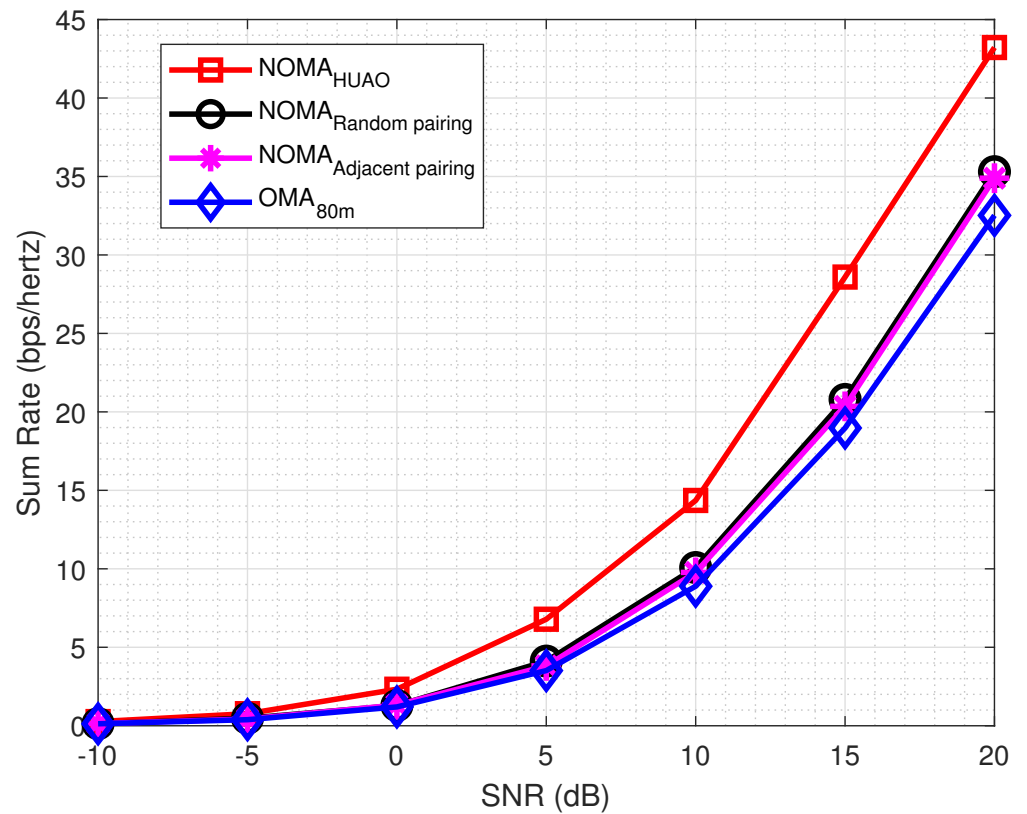


Figure 4. Comparative analysis of user pairing: suburban.

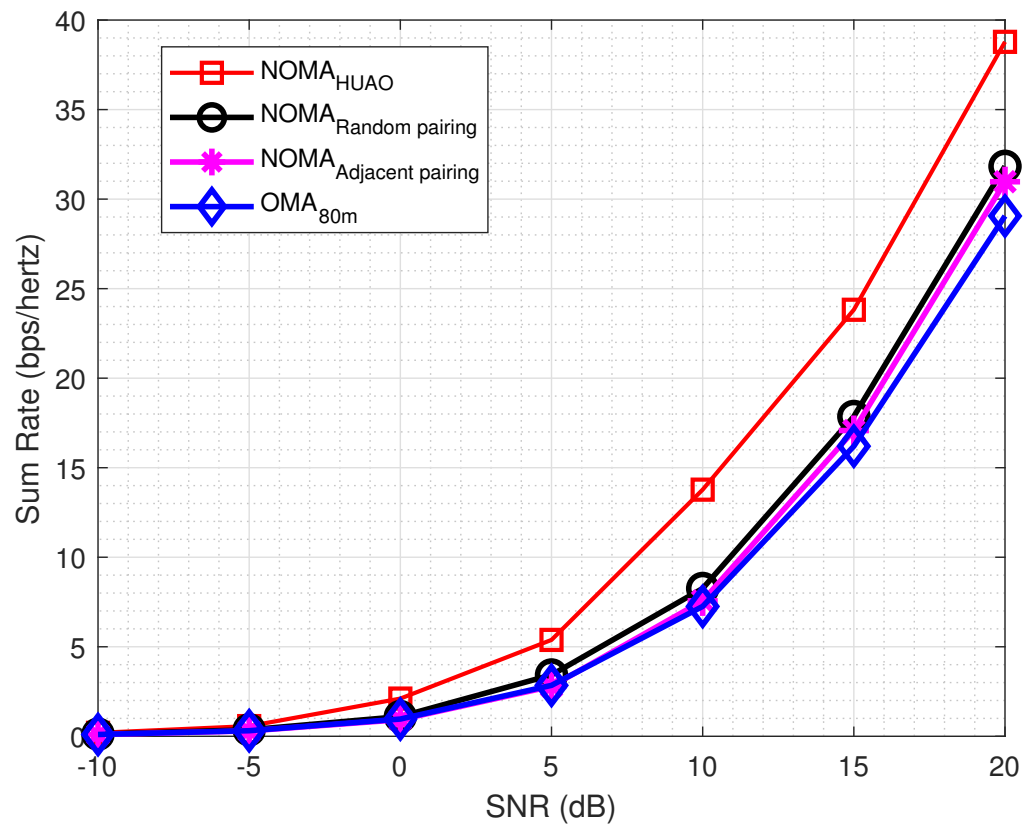


Figure 5. Comparative analysis of user pairing: urban.

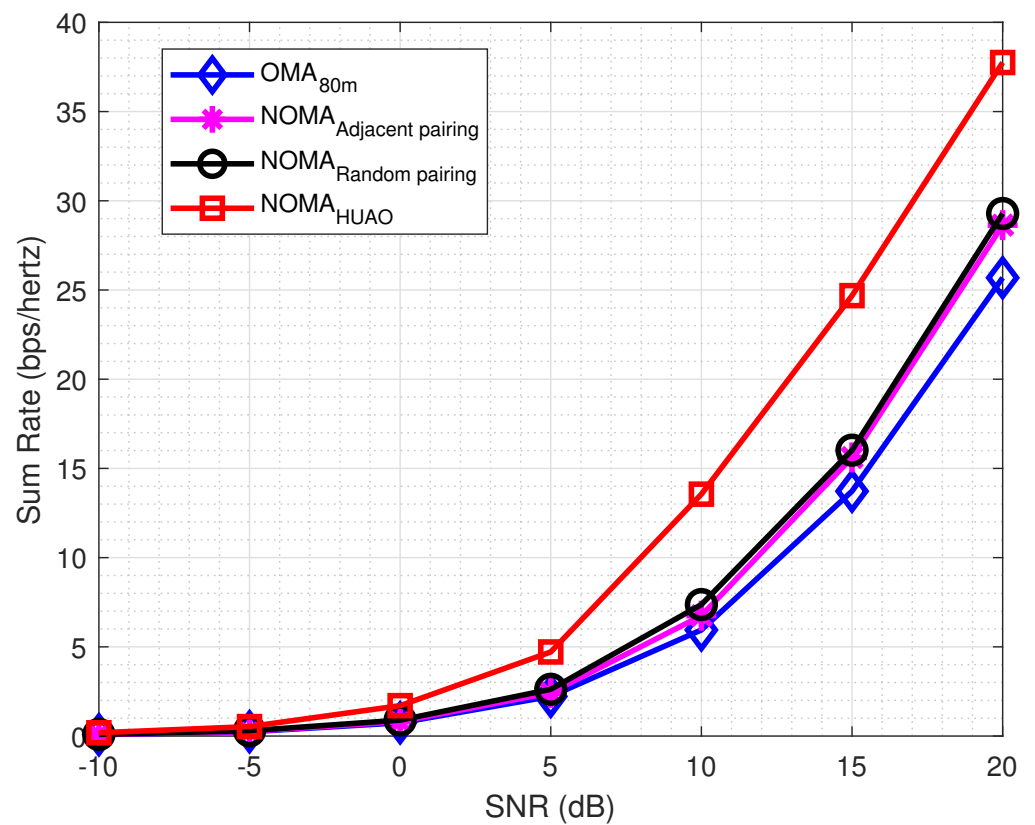


Figure 6. Comparative analysis of user pairing: dense urban.

#### 4.2. Impact of Varied SNRs: NOMA vs. OMA

The effect of different SNRs for all the environments at 80 m and 120 m is analysed in Tables 3–5. Numerical results show that the proposed HUAO-based user pairing outperforms and the performance improvement for all the environments is listed in the tables.

**Table 3.** Sum rate comparison for suburban environment.

SNR	OMA <sub>80m</sub>	OMA <sub>120m</sub>	NOMA	Percentage Improvement (80 m)	Percentage Improvement (120 m)
0	1.3964	1.2112	2.4111	42.08%	49.77%
5	3.9619	3.4893	6.7874	41.63%	48.59%
10	10.1226	8.9331	15.786	35.88%	43.41%
15	20.6275	18.9403	28.591	27.85%	33.75%
20	34.9609	32.6579	43.9261	20.41%	25.65%

**Table 4.** Sum rate comparison for urban environment.

SNR	OMA <sub>80m</sub>	OMA <sub>120m</sub>	NOMA	Percentage Improvement (80 m)	Percentage Improvement (120 m)
0	1.2376	1.152	2.1064	41.25%	45.31%
5	3.774	3.2793	5.3827	29.89%	39.08%
10	9.4486	8.6886	13.7745	31.41%	36.92%
15	20.1091	18.5457	24.8915	19.21%	25.49%
20	33.5871	31.8631	38.783	13.40%	17.84%

**Table 5.** Sum rate comparison for dense urban environment.

SNR	OMA <sub>80m</sub>	OMA <sub>120m</sub>	NOMA	Percentage Improvement (80 m)	Percentage Improvement (120 m)
0	1.259	1.0674	1.7033	26.08%	37.33%
5	3.5599	3.0732	4.7133	24.47%	34.80%
10	9.6177	8.254	13.5567	29.06%	39.11%
15	19.6127	17.8929	24.684	20.54%	27.51%
20	33.8681	31.4524	37.7492	10.28%	16.68%

#### 4.3. Impact of Environments: NOMA vs. OMA

The sum rate comparison is carried out for three different environments in Figure 7 for an altitude of 80 m for OMA-UAV. The significant performance improvement of NOMA can be seen clearly where it gives better performance for suburban environment at OMA-UAV altitude of 80 m. User pairing is optimized through PSO and the simulations show that NOMA gives performance improvement of 42% for suburban, 30.78% for urban, and 26.1% for the dense urban environment.

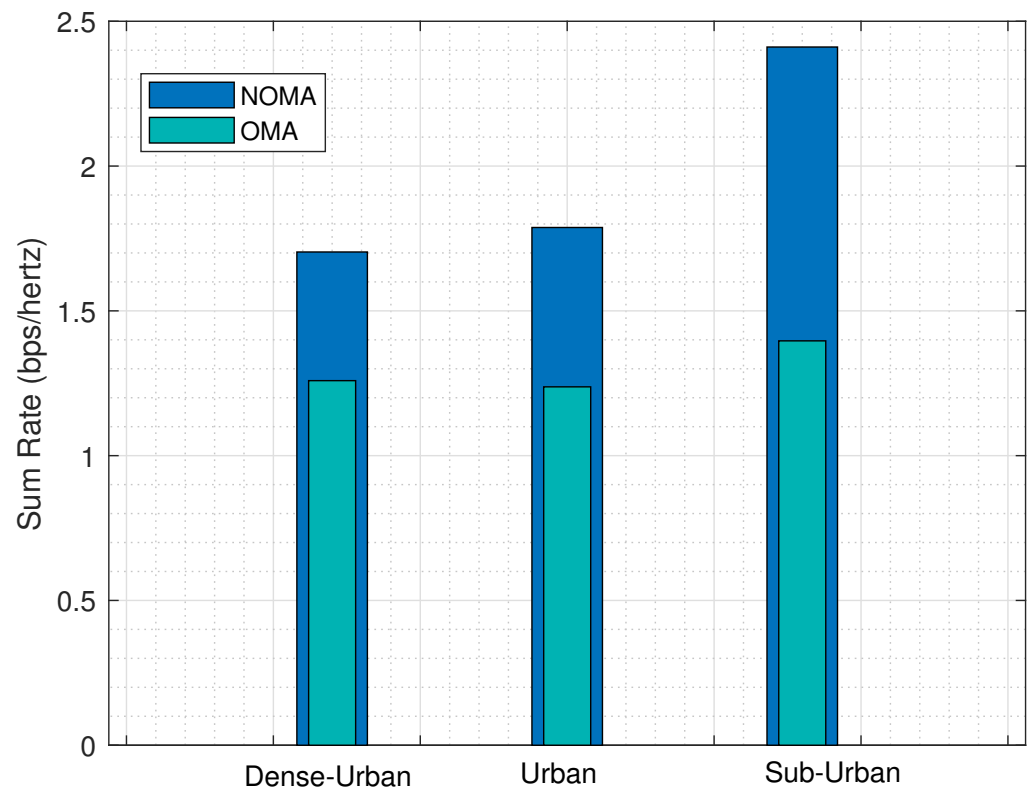


Figure 7. Sum rate comparison for different environments: OMA altitude at 80 m.

#### 4.4. Optimized NOMA Altitudes

The data rate achieved in OMA at 80 m and 120 m altitudes are taken as reference or target thresholds for the NOMA. The optimized NOMA altitudes are evaluated for the reference OMA altitudes, given in Table 6.

Table 6. Optimized NOMA altitudes.

OMA	NOMA		
	Suburban	Urban	Dense Urban
80 m	43.3014 m	94.2402 m	119.1598 m
120 m	49.7267 m	103.4393 m	158.4576 m

## 5. Conclusions

In this paper, a comparative analysis of the GA and PSO is presented for user pairing in a NOMA-based UAV communication system. The problem of joint-user pairing and altitude optimization is formulated, whereby the user pairing is done through GA and PSO, and the altitude is optimized through an interior point algorithm. The simulations prove the superiority of the proposed HUAO algorithm and PSO gives better improvement in the sum rate as compared to the GA. Sum rate performance of the suburban environment is better than the urban and dense urban environments.

**Author Contributions:** Conceptualization, M.S. and M.F.S.; Data set Generation, S.A. (Sheraz Alam) and M.J.u.R.; Funding acquisition, K.R., H.A. and S.A. (Shuja Ansari); Investigation, M.S. and S.A.G.; Methodology, M.S. and S.A.G.; Project administration, S.A.G.; Software, M.S.; Writing—original draft, M.S. and S.A.G.; Writing—review & editing, S.A. (Sheraz Alam) and M.F.S. All authors have read and agreed to the published version of the manuscript.

**Funding:** This work is also supported in parts by Engineering and Physical Sciences Research Council (Grant no. EP/X525716/1).

**Institutional Review Board Statement:** Not Applicable.

**Informed Consent Statement:** Not Applicable.

**Data Availability Statement:** Not Applicable.

**Conflicts of Interest:** The authors declare no conflict of interest.

## References

1. Khan, W.U.; Jameel, F.; Li, X.; Bilal, M.; Tsiftsis, T.A. Joint spectrum and energy optimization of NOMA-enabled small-cell networks with QoS guarantee. *IEEE Trans. Veh. Technol.* **2021**, *70*, 8337–8342. [[CrossRef](#)]
2. Huang, T.; Yang, W.; Wu, J.; Ma, J.; Zhang, X.; Zhang, D. A survey on green 6G network: Architecture and technologies. *IEEE Access* **2019**, *7*, 175758–175768. [[CrossRef](#)]
3. Nawaz, S.J.; Sharma, S.K.; Mansoor, B.; Patwary, M.N.; Khan, N.M. Non-coherent and backscatter communications: Enabling ultra-massive connectivity in 6G wireless networks. *IEEE Access* **2021**, *9*, 38144–38186. [[CrossRef](#)]
4. Mahmood, A.; Hong, Y.; Ehsan, M.K.; Mumtaz, S. Optimal resource allocation and task segmentation in iot enabled mobile edge cloud. *IEEE Trans. Veh. Technol.* **2021**, *70*, 13294–13303. [[CrossRef](#)]
5. Gupta, L.; Jain, R.; Vaszkun, G. Survey of important issues in UAV communication networks. *IEEE Commun. Surv. Tutor.* **2015**, *18*, 1123–1152. [[CrossRef](#)]
6. Khan, W.U.; Lagunas, E.; Ali, Z.; Javed, M.A.; Ahmed, M.; Chatzinotas, S.; Ottersten, B.; Popovski, P. Opportunities for physical layer security in UAV communication enhanced with intelligent reflective surfaces. *arXiv* **2022**, arXiv:2203.16907.
7. Wei, Z.; Zhu, M.; Zhang, N.; Wang, L.; Zou, Y.; Meng, Z.; Wu, H.; Feng, Z. UAV Assisted Data Collection for Internet of Things: A Survey. *IEEE Internet Things J.* **2022**, *9*, 15460–15483. [[CrossRef](#)]
8. Li, J.; Niu, Y.; Wu, H.; Ai, B.; Chen, S.; Feng, Z.; Zhong, Z.; Wang, N. Mobility Support for Millimeter Wave Communications: Opportunities and Challenges. *IEEE Commun. Surv. Tutor.* **2022**, *24*, 1816–1842. [[CrossRef](#)]
9. McEnroe, P.; Wang, S.; Liyanage, M. A Survey on the Convergence of Edge Computing and AI for UAVs: Opportunities and Challenges. *IEEE Internet Things J.* **2022**, *9*, 15435–15459. [[CrossRef](#)]
10. Mahmood, A.; Usman, M.Q.; Shahzad, K.; Saddique, N. Evolution of optimal 3D placement of UAV with minimum transmit power. *Int. J. Wirel. Commun. Mob. Comput.* **2019**, *7*, 13–18. [[CrossRef](#)]
11. Sohail, M.F.; Leow, C.Y.; Won, S. A Cat Swarm Optimization based transmission power minimization for an aerial NOMA communication system. *Veh. Commun.* **2022**, *33*, 100426. [[CrossRef](#)]
12. Zeng, Y.; Zhang, R. Energy-efficient UAV communication with trajectory optimization. *IEEE Trans. Wirel. Commun.* **2017**, *16*, 3747–3760. [[CrossRef](#)]
13. Sohail, M.F.; Leow, C.Y.; Won, S. Energy-efficient non-orthogonal multiple access for UAV communication system. *IEEE Trans. Veh. Technol.* **2019**, *68*, 10834–10845. [[CrossRef](#)]
14. Mahmood, A.; Khan, S.S.; Usman, M.Q.; Khan, S.Z.A.; Sarfaraz, M.S.; Shahzad, K.; Saddique, N. Optimal Placement of UAV for Coverage Maximization with Minimum Path Loss. *Wirel. Commun. Mob. Comput.* **2019**, *7*, 27–31. [[CrossRef](#)]
15. Khan, W.U.; Jamshed, M.A.; Mahmood, A.; Lagunas, E.; Chatzinotas, S.; Ottersten, B. Backscatter-aided NOMA V2X communication under channel estimation errors. *arXiv* **2022**, arXiv:2202.01586.
16. Ahmed, M.; Khan, W.U.; Ihsan, A.; Li, X.; Li, J.; Tsiftsis, T.A. Backscatter sensors communication for 6G low-powered NOMA-enabled IoT networks under imperfect SIC. *arXiv* **2021**, arXiv:2109.12711.
17. Islam, S.R.; Avazov, N.; Dobre, O.A.; Kwak, K.S. Power-domain non-orthogonal multiple access (NOMA) in 5G systems: Potentials and challenges. *IEEE Commun. Surv. Tutor.* **2016**, *19*, 721–742. [[CrossRef](#)]
18. Khan, W.U.; Lagunas, E.; Mahmood, A.; Chatzinotas, S.; Ottersten, B. Integration of backscatter communication with multi-cell NOMA: A spectral efficiency optimization under imperfect SIC. *arXiv* **2021**, arXiv:2109.11509.
19. Wang, K.; Li, H.; Ding, Z.; Xiao, P. Reinforcement learning based latency minimization in secure NOMA-MEC systems with hybrid SIC. *IEEE Trans. Wirel. Commun.* **2022**. [[CrossRef](#)]
20. Li, X.; Liu, M.; Deng, C.; Mathiopoulos, P.T.; Ding, Z.; Liu, Y. Full-duplex cooperative NOMA relaying systems with I/Q imbalance and imperfect SIC. *IEEE Wirel. Commun. Lett.* **2019**, *9*, 17–20. [[CrossRef](#)]
21. Khan, W.U.; Jamshed, M.A.; Lagunas, E.; Chatzinotas, S.; Li, X.; Ottersten, B. Energy efficiency optimization for backscatter enhanced NOMA cooperative V2X communications under imperfect CSI. *IEEE Trans. Intell. Transp. Syst.* **2022**. [[CrossRef](#)]
22. Ali, Z.; Khan, W.U.; Ihsan, A.; Waqar, O.; Sidhu, G.A.S.; Kumar, N. Optimizing resource allocation for 6G NOMA-enabled cooperative vehicular networks. *IEEE Open J. Intell. Transp. Syst.* **2021**, *2*, 269–281. [[CrossRef](#)]
23. Nawaz, H.; Ali, H.M.; Laghari, A.A. UAV communication networks issues: A review. *Arch. Comput. Methods Eng.* **2021**, *28*, 1349–1369. [[CrossRef](#)]
24. Sohail, M.F.; Leow, C.Y. Maximized fairness for NOMA based drone communication system. In Proceedings of the 2017 IEEE 13th Malaysia International Conference on Communications (MICC), Johor Bahru, Malaysia, 28–30 November 2017; pp. 119–123.
25. He, H.; Zhang, S.; Zeng, Y.; Zhang, R. Joint altitude and beamwidth optimization for UAV-enabled multiuser communications. *IEEE Commun. Lett.* **2017**, *22*, 344–347. [[CrossRef](#)]

26. Cicek, C.T.; Kutlu, T.; Gultekin, H.; Tavli, B.; Yanikomeroglu, H. Backhaul-aware placement of a UAV-BS with bandwidth allocation for user-centric operation and profit maximization. *arXiv* **2018**, arXiv:1810.12395.
27. Duan, R.; Wang, J.; Jiang, C.; Yao, H.; Ren, Y.; Qian, Y. Resource allocation for multi-UAV aided IoT NOMA uplink transmission systems. *IEEE Internet Things J.* **2019**, *6*, 7025–7037. [[CrossRef](#)]
28. Amantayeva, A.; Yerzhanova, M.; Kizilirmak, R.C. UAV location optimization for UAV-to-vehicle multiple access channel with visible light Communication. In Proceedings of the 2019 Wireless Days (WD), Manchester, UK, 24–26 April 2019; pp. 1–4.
29. Zhong, X.; Guo, Y.; Li, N.; Chen, Y.; Li, S. Deployment optimization of UAV relay for malfunctioning base station: Model-free approaches. *IEEE Trans. Veh. Technol.* **2019**, *68*, 11971–11984. [[CrossRef](#)]
30. Chowdhury, M.M.U.; Bulut, E.; Guvenc, I. Trajectory optimization in UAV-assisted cellular networks under mission duration constraint. In Proceedings of the 2019 IEEE Radio and Wireless Symposium (RWS), Orlando, FL, USA, 20–23 January 2019; pp. 1–4.
31. Mounchili, S.; Hamouda, S. New user grouping scheme for better user pairing in NOMA systems. In Proceedings of the 2020 International Wireless Communications and Mobile Computing (IWCMC), Limassol, Cyprus, 15–19 June 2020; pp. 820–825.
32. Mounchili, S.; Hamouda, S. Efficient pairing distance for better radio capacity in noma systems. In Proceedings of the 2020 4th International Conference on Advanced Systems and Emergent Technologies (IC\_ASET), Hammamet, Tunisia, 15–18 December 2020; pp. 383–388.
33. Chinnadurai, S.; Selvaprabhu, P.; Lee, M.H. A novel joint user pairing and dynamic power allocation scheme in MIMO-NOMA system. In Proceedings of the 2017 International Conference on Information and Communication Technology Convergence (ICTC), Jeju, Korea, 18–20 October 2017; pp. 951–953.
34. Shahab, M.B.; Kader, M.F.; Shin, S.Y. A virtual user pairing scheme to optimally utilize the spectrum of unpaired users in non-orthogonal multiple access. *IEEE Signal Process. Lett.* **2016**, *23*, 1766–1770. [[CrossRef](#)]
35. Mouni, N.S.; Kumar, A.; Upadhyay, P.K. Adaptive user pairing for NOMA systems with imperfect SIC. *IEEE Wirel. Commun. Lett.* **2021**, *10*, 1547–1551. [[CrossRef](#)]
36. Azam, I.; Shahab, M.B.; Shin, S.Y. User pairing and power allocation for capacity maximization in uplink NOMA. In Proceedings of the 2019 42nd International Conference on Telecommunications and Signal Processing (TSP), Budapest, Hungary, 1–3 July 2019; pp. 690–694.
37. Nasser, A.; Muta, O.; Gacanin, H.; Elsabrouty, M. Joint user pairing and power allocation with compressive sensing in NOMA systems. *IEEE Wirel. Commun. Lett.* **2020**, *10*, 151–155. [[CrossRef](#)]
38. Sohail, M.F.; Leow, C.Y.; Won, S. Non-orthogonal multiple access for unmanned aerial vehicle assisted communication. *IEEE Access* **2018**, *6*, 22716–22727. [[CrossRef](#)]
39. Khan, W.U.; Liu, J.; Jameel, F.; Khan, M.T.R.; Ahmed, S.H.; Jäntti, R. Secure backscatter communications in multi-cell NOMA networks: Enabling link security for massive IoT networks. In Proceedings of the IEEE INFOCOM 2020-IEEE Conference on Computer Communications Workshops (INFOCOM WKSHPS), Toronto, ON, Canada, 6–9 July 2020; pp. 213–218.
40. Mahmood, A.; Ahmed, A.; Naeem, M.; Amirzada, M.R.; Al-Dweik, A. Weighted utility aware computational overhead minimization of wireless power mobile edge cloud. *Comput. Commun.* **2022**, *190*, 178–189. [[CrossRef](#)]
41. Mohammed, A.; Mehmood, A.; Pavlidou, F.N.; Mohorcic, M. The role of high-altitude platforms (HAPs) in the global wireless connectivity. *Proc. IEEE* **2011**, *99*, 1939–1953. [[CrossRef](#)]
42. Khan, W.U.; Ihsan, A.; Nguyen, T.N.; Javed, M.A.; Ali, Z. NOMA-enabled backscatter communications for green transportation in automotive-Industry 5.0. *IEEE Trans. Ind. Inform.* **2022**. [[CrossRef](#)]